Published in final edited form as:
Int J Radiat Oncol Biol Phys. 2011 February 1; 79(2): 531–539. doi:10.1016/j.ijrobp.2010.08.044.

CELL-SPECIFIC RADIOSENSITIZATION BY GOLD NANOPARTICLES AT MEGAVOLTAGE RADIATION ENERGIES

Suneil Jain, M.B., B.Ch.[*,†], **Jonathan A. Coulter, Ph.D.**[‡], **Alan R. Hounsell, Ph.D.**[§], **Karl T. Butterworth, Ph.D.**[†], **Stephen J. McMahon, Ph.D.**[¶], **Wendy B. Hyland, B.Sc. Hons.**[¶], **Mark F. Muir, B.Sc.**[¶], **Glenn R. Dickson, Ph.D.**[†], **Kevin M. Prise, Ph.D.**[†], **Fred J. Currell, Ph.D.**[¶], **Joe M. O'Sullivan, M.D.**[*], and **David G. Hirst, Ph.D.**[‡]

[*]Northern Ireland Cancer Centre, Queen's University, Belfast, Northern Ireland [†]Centre for Cancer Research and Cell Biology, School of Medicine, Queen's University, Belfast, Northern Ireland [‡]Experimental Therapeutics Research Group, School of Pharmacy, Queen's University, Belfast, Northern Ireland [§]Medical Physics Agency, Northern Ireland Cancer Centre, Queen's University, Belfast, Northern Ireland [¶]Atomic and Molecular Physics Group, International Research Centre for Experimental Physics, Queen's University, Belfast, Northern Ireland

Abstract

Purpose—Gold nanoparticles (GNPs) have been shown to cause sensitization with kilovoltage (kV) radiation. Differences in the absorption coefficient between gold and soft tissue, as a function of photon energy, predict that maximum enhancement should occur in the kilovoltage (kV) range, with almost no enhancement at megavoltage (MV) energies. Recent studies have shown that GNPs are not biologically inert, causing oxidative stress and even cell death, suggesting a possible biological mechanism for sensitization. The purpose of this study was to assess GNP radiosensitization at clinically relevant MV X-ray energies.

Methods and Materials—Cellular uptake, intracellular localization, and cytotoxicity of GNPs were assessed in normal L132, prostate cancer DU145, and breast cancer MDA-MB-231 cells. Radiosensitization was measured by clonogenic survival at kV and MV photon energies and MVelectron energies. Intracellular DNA double-strand break (DSB) induction and DNA repair were determined and GNP chemosensitization was assessed using the radiomimetic agent bleomycin.

Results—GNP uptake occurred in all cell lines and was greatest in MDA-MB-231 cells with nanoparticles accumulating in cytoplasmic lysosomes. In MDA-MB-231 cells, radiation sensitizer enhancement ratios (SERs) of 1.41, 1.29, and 1.16 were achieved using 160 kVp, 6 MV, and 15 MV X-ray energies, respectively. No significant effect was observed in L132 or DU145 cells at kV or MV energies (SER 0.97-1.08). GNP exposure did not increase radiation-induced DSB formation or inhibit DNA repair; however, GNP chemosensitization was observed in MDA-MB-231 cells treated with bleomycin (SER 1.38).

Conclusions—We have demonstrated radiosensitization in MDA-MB-231 cells at MV X-ray energies. The sensitization was cell-specific with comparable effects at kV and MV energies, no increase in DSB formation, and GNP chemopotentiation with bleomycin, suggesting a possible biological mechanism of radiosensitization.

Reprint requests: Suneil Jain, M.B., B.Ch., Northern Ireland Cancer Centre, 51 Lisburn Road, Belfast, Northern Ireland BT97AB. Tel: +442890972012; Fax: +442890309106; suneiljain@hotmail.com.

Conflict of interest: none.

Europe PMC Funders Author Manuscripts

Keywords

Gold nanoparticles; Radiosensitizers; Chemoradiation; Nanotechnology; DNA repair

INTRODUCTION

There is increasing evidence that combining radiation therapy with systemic drugs, such as cytotoxic chemotherapy or biological agents, improves survival in cancer patients (1). Gold nanoparticles (GNPs) have been shown to sensitize cancer cells to kilovoltage radiation *in vitro* and *in vivo* (2, 3). GNPs have properties that make them attractive for use in cancer therapy including small size, biocompatibility, and passive accumulation in tumors because of the enhanced permeability and retention effect (4). Furthermore, GNPs can be functionalized with antibodies or other proteins to actively target tumor cells and intracellular targets, such as the nucleus (5, 6). Because of the high atomic number (Z) of gold, GNPs can be used as a contrast agent, potentially aiding image-guided radiotherapy and enabling quantification of intratumoral GNP dose (7).

Although the concentration and preparation of GNPs have varied in published studies, kV radiosensitization has usually been attributed to increased photon absorption in high-Z materials, such as gold, compared with soft tissue. The photoelectric effect is dominant at kV energies in which photon absorption has a $\sim Z^4$ relationship with target material. *In vitro* radiosensitization and *in vivo* tumor growth delay coupled with improved survival have been demonstrated using GNPs (3, 8).

Although some cancer patients are treated at kV energies with brachytherapy (*e.g.*, Iodine-125, 35.5 keV), unsealed radioisotopes, or intraoperative radiotherapy, megavoltage (MV) X-rays are essential for most radical radiotherapy regimes to provide both skin sparing and adequate dose deposition to central tumors (9). Monte Carlo (MC) modeling has predicted much lower physical dose enhancement with GNPs at MV energies in which Compton effects, which have no relationship with Z, are dominant. For instance, Cho *et al.* predicted dose enhancement factors (DEFs) of 2.11 for 7 mg Au/g tumor with 140 kVp X-rays and 1.007 for 6 MV energies (10). An alternative mechanism has been proposed through work in DNA plasmid models, in which sensitization occurs by short-range electrons with energies of 200 eVor less. Because these low-energy electrons are produced by target interactions with any photon energy, GNP-mediated sensitization would be predicted to occur even with MV photons (11).

Recent studies demonstrate that GNPs, although biocompatible, are not inert, causing reactive oxygen species (ROS) production, cytotoxicity, cytokinesis arrest, and apoptosis (12, 13). Metal compounds, such as cisplatin, have been shown to cause radiosensitization from the inhibition of DNA repair (14). To date, possible biological mechanisms of GNP radiosensitization have not been fully investigated.

Given the emerging evidence of biological interactions with GNPs the purpose of this study was to examine *in vitro* radiosensitization with clinically relevant MV photons and electrons in human cancer and normal cells. We also investigated the role of DNA repair, DSB formation, cell-cycle regulation, and GNP chemosensitization using the radiomimetic agent bleomycin.

Europe PMC Funders Author Manuscripts

METHODS AND MATERIALS

Gold nanoparticles

Spherical 1.9-nm GNPs (Aurovist) used in previous radiation studies were purchased from Nanoprobes Inc. (Yaphank, NY) (3, 8). GNPs were suspended in sterile water (Sigma, UK), filtered through a 0.2 μm filter and stored at −20°C per manufacturer's instructions. This stock solution was diluted in culture media immediately before use.

Cell culture

DU145 human prostate cancer cells, MDA-MB-231 breast cancer cells, and L132 lung epithelial cells were cultured in Roswell Park Memorial Institute 1640, Dulbecco modified eagle medium, and minimum essential medium, respectively. All media were supplemented with 10% fetal bovine serum and 1% penicillin-streptomycin (Invitrogen, UK). Cells were maintained in a tissue culture incubator at 37°C with 5% CO_2/95% air.

Transmission electron microscopy

A total of 1.5×10^5 cells were plated for 24 h, then exposed to GNPs for a further 24 h. Cells were washed twice in phosphate-buffered saline (PBS), trypsinized, pelleted, and fixed in 4% gluteraldehyde in 0.1M sodium cocodylate. Cells were postfixed in 1% osmium tetroxide, dehydrated in ethanol, and embedded in agar resin. Sections of 60–70 nm were cut using an ultramicrotome, placed on copper grids, stained with uranyl acetate and lead citrate, and imaged with an FEI Technai F20 transmission electron microscopy (Hillsboro, OR).

Inductively coupled plasma–atomic emission spectroscopy

A total of 7.5×10^4 cells were plated for 24 h then exposed to GNPs for 24 h, washed three times in PBS, trypsinized, counted, and digested in *aqua regia*. Gold content was determined using a Perkin Elmer Optima 4300 DV Inductively Coupled Plasma Optical Emission Spectrometer (Shelton, CT).

Clonogenic survival assays

A total of 7.5×10^4 cells were plated in 35 mm^2 dishes for 24 h, exposed to GNPs for 24 h, then irradiated with 0–6 Gy X-rays or electrons. Cells were washed twice in PBS, trypsinized, counted, replated in six-well plates, and incubated for 9–14 days. Colonies were stained with 0.4% crystal violet and counted using a Colcount colony counter (Oxford Optronix, UK). For delayed plating experiments, fully confluent cells were exposed to GNPs for 24 h then irradiated with 4 Gy 160 kVp X-rays and plated 0–6 h after irradiation as discussed previously. For split-dose recovery, cells received two fractions of 2 Gy 0–6 h apart and were plated as discussed previously. For chemotherapy studies, bleomycin sulphate (Sigma, UK) was dissolved in sterile water and further diluted in culture medium. Cells were treated with GNP for 24 h, bleomycin was added for a further 3 h, and cells were plated as discussed previously.

Surviving fractions (SF) were calculated relative to nonirradiated cells and fitted to the linear quadratic equation $S = \exp(-\alpha D - \beta D^2)$ using least-squares regression in Prism 5.0 (GraphPad Software, CA). The area under the curve, which represents the mean inactivation dose (MID), was obtained and the sensitizer enhancement ratio (SER) calculated by dividing the MID of nonexposed cells with gold-exposed cells as published (15).

53BP1 foci immunofluorescence

Cells were exposed to GNP for 24 h, irradiated with 0–1 Gy of 160 kVp X-rays, washed twice in PBS, fixed with 50% methanol:50% acetone, and permeabilized in 0.5% triton

X-100 (Sigma, UK). After overnight incubation in blocking buffer (PBS, 0.1% triton, 5% horse serum, 0.2% milk), cells were incubated with rabbit anti-53BP1 antibody (Abcam, UK) at 1:2000 concentration and incubated with secondary anti-rabbit Alexa fluor-488 (Invitrogen, UK). Nuclei were counterstained with 4,6-diamidino-2-phenylindole (0.1 μg/mL). Foci were counted using a fluorescence microscope (Zeiss Axiovert 200M, UK); typically 100 cells were counted per sample.

Cell-cycle analysis by flow cytometry

A total of 7.5×10^4 cells were plated in 35 mm^2 dishes for 24 h, exposed to GNPs in culture medium for 24 h, trypsinized, centrifuged, and fixed in 70% ethanol at 4°C for 1 h. Cells were resuspended in PBS containing 50 μg mL propidium iodide and 10 μg mL RNase and incubated at 37°C for 30 minutes. Samples were analyzed using a FACSCalibur flow cytometer and CELL-Quest software (Becton-Dickson, UK).

Irradiation setup

Megavoltage X-ray (6 MV, 15 MV) and electron (6 MeV, 16 MeV) irradiations were performed using a Varian 2100CD linear accelerator (LINAC) with a dosimetric calibration traceable to the National Physical Laboratory, Teddington, UK. The 35 mm^2 dishes contained a layer of cells plus approximately 2 mm of medium. The remaining 8 mm depth of the dish was air filled. For the X-ray setup, irradiations were performed at 100-cm focus to surface distance using a 15 cm × 15 cm field size at 5 cm deep from below. Six centimeters of water-equivalent back-scatter material was placed on top of the dishes containing the cells. The dose-rates at the position of the cells were 3.55 Gy/min and 3.85 Gy/min for 6 MV and 15 MV, respectively. For the electron setup, irradiations were performed from above using a 15 cm × 15 cm applicator at a depth of 1 cm to the top of dish. The cells were set to 100 cm from the electron source. The dose-rate was 4.0 Gy/min for both 6 MeV and 16 MeV. Because of the air gaps within and between the dishes, dosimetric verification was undertaken using Gafchromic film (ISP Corp., Wayne, NJ) on two separate occasions. The measured dose was found to be within 5.5% of that calculated for all irradiations. The 160-kVp irradiations were performed using a Faxitron CP-160 X-ray generator with 35 mm^2 dishes positioned as described previously with a focus to surface distance of 30 cm^2 and a dose rate of 0.69 Gy/min.

Statistical analysis

All experiments were carried out in triplicate with results expressed as mean ± standard error (SE). Statistically significant differences were calculated using the two-tailed unpaired *t*-test or one-way analysis of variance with a p value of ≤ 0.05 considered significant. To assess correlation r^2 values were calculated from the Pearson correlation coefficient using Prism 5.0 (GraphPad Software, CA).

RESULTS

GNP uptake and cellular toxicity

TEM demonstrated that GNPs accumulated in cytoplasmic lysosomes, where they appeared aggregated (Fig. 1a). After 24 h exposure to 12 μM GNP, cellular uptake was greatest in MDA-MB-231 cells with least uptake observed in L132 cells (Fig. 1b).

Using clonogenic survival assays a reduction in SF in all cell lines exposed to GNPs for 24 h was observed the degree of which was cell-type dependent. Loss of clonogenicity was maximal in the MDA-MB-231 cell line with a 19.4% reduction in survival (Fig. 1c). There was a significant correlation between GNP uptake and cytotoxicity with an r^2 value of 0.97 ($p = 0.015$).

kV radiosensitization increases with GNP concentration

To determine an appropriate GNP concentration for further radiation experiments, the effect of increasing GNP concentration on radiosensitization to 160 kVp X-rays in MDA-MB-231 cells was assessed. Figure 2 shows the ratio of surviving fractions after 0 Gy and 4 Gy (SF_0 and SF_4, respectively) with increasing GNP concentrations relative to the ratio of SF_0 to SF_4 in control samples. The GNP sensitizing effect reached a plateau at a concentration of 12 μM and did not increase further with higher concentrations. Based on these results, all further experiments were carried out at 12 μM GNP concentrations with 24 hour incubation.

Radiosensitization is cell line–specific and occurs at megavoltage photon energies

Initially, radiosensitization was examined at kV energies with 160 kVp X-rays, where the greatest physical dose enhancement would be expected to occur (10). In MDA-MB-231 cells significant radiosensitization occurred at 160 kVp X-rays with a SER of 1.41 ($p = 0.005$) (Fig. 3). The SF_4 reduced from 0.38 in controls to 0.15 in cells exposed to GNP for 24 h before irradiation ($p = 0.001$). An increase in both the α and β components of the linear quadratic curve was observed (Table 1). Surprisingly, no significant radiosensitization was observed in DU145 or L132 cells despite GNP uptake occurring in both cell lines (SER 0.92 and 1.05). There was no significant correlation between GNP uptake and radiosensitization with an r^2 value of 0.35 ($p = 0.41$).

In view of the clinical importance of MV radiation therapy, GNP sensitization using MV photons produced by a LINAC was assessed. Interestingly, similar radiosensitization was observed with 6 and 15 MV photons in MDA-MB-231 cells with SERs of 1.29 ($p = 0.002$) and 1.16 ($p = 0.19$), respectively. Although the SER was slightly lower at MV energies, there was no significant difference in MIDs compared with 160 kVp, where a SER of 1.41 was achieved ($p = 0.75$). SF_4 values reduced from 0.28 in control cells to 0.12 in GNP exposed cells at 6 MV ($p = 0.001$). No significant effect observed in DU145 or L132 cells with 6 MV photons (SER 1.13 and 1.08). Table 1 summarizes the SERs of all cell lines and the α, β, and SF_4 values for MDA-MB-231 cells.

Cell line–specific sensitization with megavoltage electrons

In view of the sensitization observed with MV photons, we assessed effects with MVelectrons to eliminate the effect of primary photon interactions with GNPs. Sensitization was observed in MDA-MB-231s at 16 MeV electron energies with an SER of 1.35 ($p = 0.01$) (Fig. 4). No statistically significant difference was observed at 6 MeV energies (SER 1.04, $p = 0.64$); however, there was a reduction in survival in GNP exposed cells at higher radiation doses with SF_6 values reduced from 0.078 to 0.023 ($p = 0.0001$). As in the photon irradiation experiments, sensitization was not observed in DU145 or L132 cells.

GNPs sensitize MDA-MB-231 cells to the radiomimetic drug bleomycin

The sensitizing effects of GNPs with MV radiation in MDA-MB-231 cells were larger than predicted by MC simulations of dose enhancement. GNP sensitization was therefore assessed in a model where the physical effects of radiation were not present using bleomycin, which causes DNA DSBs and has been used as a radiomimetic in previous studies (16). Sensitization was observed at all bleomycin doses with an SER of 1.38 (Fig. 5). At a concentration of 5 μg/mL, a SF of 0.62 was observed in bleomycin-only controls and 0.39 in cells exposed to GNPs before bleomycin exposure.

GNPs do not inhibit DNA repair or increase DNA DSB formation

A common mechanism of biological radiosensitization is inhibition of DNA repair, as demonstrated with cisplatin (14). In the present study, there was no inhibition of DNA

damage repair by GNPs in either split-dose recovery or delayed plating experiments in MDA-MB-231 cells (Fig. 6a,c). Furthermore, there was no significant difference in 53BP1 foci, a marker of DSB formation, 1 h or 24 h after irradiation in this cell line, suggesting no increase in DNA damage or inhibition of repair in GNP treated cells (Fig. 6b).

GNPs do not cause cell-cycle synchronization

Some radiosensitizing drugs cause cells to accumulate in the radiosensitive G2/M phase of the cell cycle (17). In this study, flow cytometry showed no cell-cycle synchronization or accumulation of MDA-MB-231 cells in G2/M after 24 h exposure to 12 μM GNPs (Fig. 6d).

DISCUSSION

In agreement with other studies, GNP cellular uptake and localization in cytoplasmic endosomes occurred in all cells (18). Although there have been conflicting reports of GNP cytotoxicity there is increasing evidence that GNPs are not biologically inert, and it is likely this contributes to sensitization observed in this study. Cell-selective GNP cytotoxicity and apoptosis with 33 nm GNPs has previously been described with greater effects observed in A549 human lung cancer cell lines than in BHK 21 normal kidney cells (19). Kang *et al.* used 30-nm GNPs functionalized with nuclear localization signals, demonstrating cancer cell–specific DNA DSB formation, cytokinesis arrest, and apoptosis in the absence of radiation (13). Pan *et al.* demonstrated cytotoxicity, necrosis, mitochondrial toxicity, ROS production, and oxidative stress-associated gene upregulation with 1.4 nm GNPs in Hela cells (12). A recent study combined 15 nm citrate-capped GNPs with the ROS-producing agent 5-aminolevulinic acid. GNPs alone did not produce ROS nor cause cell cytotoxicity in breast cancer MCF-7 cells; however, they appeared to catalyze agent 5-aminolevulinic acid–induced ROS production and cytotoxicity, effects that were abrogated by free radical inhibitors (20).

KV radiosensitization was observed in MDA-MB-231 cells with a SER of 1.41, but not in DU145 or L132 cells despite GNP uptake occurring in all three cell lines, albeit to a lesser extent than in MDA-MB-231 cells. Rahman *et al.* using the same 1.9 nm GNPs at 0.5 mM and 1 mM concentrations demonstrated dose enhancement factors of 1.4 and 2.2, respectively, using a cell proliferation assay with 150 kVp X-rays in bovine aortic endothelial cells (8). In agreement with our results, Chithrani *et al.* obtained a DEF of 1.43 with a lower concentration (1×10^{-3}%) of 50 nm citrate coated GNPs and 220 kVp X-rays (21).

In addition, GNP radiosensitization was observed in MDA-MB-231 cells at 6 MV and 15 MV photon energies. Two recent studies have reported *in vitro* GNP sensitization at MV photon energies. One study used Hela cells exposed to 50 nm citrate-coated GNPs for 24 h with DEFs of 1.66, 1.43, and 1.17 observed with 105 kVp, 220 kVp, and 6 MV X-rays, respectively (21). As with our study, the enhancement was less at MV energies, but far greater than MC simulations predict. A further study used CT26 murine cancer cells treated with high concentrations (500 μM) of 6.1 nm pegylated GNPs for 48 h. Cells were irradiated with 8 keV, 160 kVp, and 6 MV X-rays achieving a DEF of ~1.44, 1.1, and 1.32, respectively (22). Radiosensitization with MV electrons has been noted in other studies with Rahman *et al.* reporting DEFs of 2.9 and 3.7 using 0.5 mM concentrations of 1.9 nm GNPs at 6 MeV and 12 MeV electron energies (8).

It is well established that the primary target of radiation is nuclear DNA, with DSB formation being the most lethal DNA damage lesion; however, evidence is increasing that radiation damage to mitochondria and the cell membrane may contribute to the cytotoxic effect of radiation (23). Many commonly used radiosensitizing agents increase DNA DSB

break formation or inhibit DNA repair (14). Other sensitizers target radioresistance pathways such as Ras or the epidermal growth factor receptor or specifically target hypoxic cells (24, 25). Established chemotherapeutic agents including docetaxel have been shown to cause radiosensitization by increasing cellular apoptosis and synchronizing cells in the radiosensitive G2/M phase of the cell cycle (17). Novel agents, such as the antisense oligodeoxynucleotide oblimersen, inhibit the antiapoptotic protein bcl-2, increasing apoptosis and causing radiosensitization (26). In this work, there was no evidence that GNPs increased radiation-induced DSBs; furthermore, cell-cycle progression was not affected and no inhibition of DNA damage repair was observed. One study observed an increase in DSB formation using 50 nm citrate coated GNPs in Hela cells irradiated with 6 MV photons (21). In another study, 10.8 nm glucose capped GNPs activated cyclin-dependent kinases, leading to accumulation in the G2/M phase of the cell cycle and thereby causing radiosensitization at nM GNP concentrations (27).

In this work, bleomycin, known to cause DSBs, was used as a radiomimetic agent to assess sensitization when the physical interactions of radiation with matter were not present. Bleomycin has been shown to complex with metal ions leading to oxygen radical formation and DNA damage (28). In murine lung epithelial cells, bleomycin has been shown to produce ROS leading to mitochondrial leakage and apoptosis, which can be inhibited by the free radical scavenger glutathione (29).

GNP kV sensitization has been demonstrated using many different sizes and preparations of GNP and evidence is emerging for significant effects at MV energies. The importance of primary radiation absorption in GNPs and deposition of that energy in target tissue needs to be clarified. This could be accurately quantified using monochromatic X-rays produced by a synchrotron, and this work is under way in our group. Similarly, the role of low-energy electron and nanoscale dose deposition needs to be further explored through more advanced MC modeling. If sensitization is primarily an effect of biological interactions with GNPs, the importance of GNP ROS production, hypoxia, and cell signaling pathways need to be elucidated. The first in human Phase I clinical trial of targeted GNPs has recently reported (30). There is a pressing need for more *in vivo* radiation studies, particularly with targeted GNPs with a view to translating this work to clinical trials.

CONCLUSION

This study demonstrates that commercially available 1.9 nm GNPs are taken up by cancer cells, localize in cytoplasmic lysosomes, and cause radiosensitization with kVand MV photons in MDA-MB-231 breast cancer cells. Sensitization was cell specific, occurring in MDA-MB-231, cells but not in DU145 or L132 cells despite GNP uptake occurring in these cell lines. In addition, MDA-MB-231 cell sensitization was observed at kV and MV photon energies and also with MV electrons, which is not consistent with predictions from MC modeling (10). Furthermore, no increase in DNA DSB formation was observed, as would be expected if enhancement was simply from an increase in radiation dose absorption. GNPs were also shown to potentiate the effect of the radiomimetic agent bleomycin in the absence of radiation, suggesting biological interactions of GNPs with cells could be the main mechanism by which sensitization occurred in this study.

Acknowledgments

Supported by Men Against Cancer and Cancer Research UK (grant number C1278/A990 to D.G.H. and C1513/A7047 to K.M.P.).

REFERENCE

1. Bernier J. Current state-of-the-art for concurrent chemoradiation. Semin Radiat Oncol. 2009; 19:3–10. [PubMed: 19028339]
2. Kong T, Zeng J, Wang X, et al. Enhancement of radiation cytotoxicity in breast-cancer cells by localized attachment of gold nanoparticles. Small. 2008; 4:1537–1543. [PubMed: 18712753]
3. Hainfeld JF, Slatkin DN, Smilowitz HM. The use of gold nano-particles to enhance radiotherapy in mice. Phys Med Biol. 2004; 49:N309–N315. [PubMed: 15509078]
4. Maeda H. The enhanced permeability and retention (EPR) effect in tumor vasculature: The key role of tumor-selective macromolecular drug targeting. Adv Enzyme Regul. 2001; 41:189–207. [PubMed: 11384745]
5. Jiang W, Kim YS, Rutka JT, Chan CW. Nanoparticle-mediated cellular response is size-dependent. Nat Nano. 2008; 3:145–150.
6. Nativo P, Prior IA, Brust M. Uptake and intracellular fate of surface-modified gold nanoparticles. ACS Nano. 2008; 2:1639–1644. [PubMed: 19206367]
7. Hainfeld JF, Slatkin DN, Focella TM, et al. Gold nanoparticles: A new X-ray contrast agent. Br J Radiol. 2006; 79:248–253. [PubMed: 16498039]
8. Rahman WN, Bishara N, Ackerly T, et al. Enhancement of radiation effects by gold nanoparticles for superficial radiation therapy. Nanomedicine. 2009; 5:136–142. [PubMed: 19480049]
9. McMahon SJ, Mendenhall MH, Jain S, et al. Radiotherapy in the presence of contrast agents: A general figure of merit and its application to gold nanoparticles. Phys Med Biol. 2008; 53:5635–5651. [PubMed: 18812647]
10. Cho SH. Estimation of tumour dose enhancement due to gold nanoparticles during typical radiation treatments: A preliminary monte carlo study. Phys Med Biol. 2005; 50:N163–N173. [PubMed: 16030374]
11. Zheng Y, Hunting DJ, Ayotte P, et al. Radiosensitization of DNA by gold nanoparticles irradiated with high-energy electrons. Radiat Res. 2008; 169:19–27. [PubMed: 18159957]
12. Pan Y, Leifert A, Ruau D, et al. Gold nanoparticles of diameter 1.4 nm trigger necrosis by oxidative stress and mitochondrial damage. Small. 2009; 5:2067–2076. [PubMed: 19642089]
13. Kang B, Mackey MA, El-Sayed MA. Nuclear targeting of gold nanoparticles in cancer cells induces DNA damage, causing cytokinesis arrest and apoptosis. J Am Chem Soc. 2010; 132:1517–1519. [PubMed: 20085324]
14. Marcu L, van Doorn T, Olver I. Cisplatin and radiotherapy in the treatment of locally advanced head and neck cancer. Acta Oncol. 2003; 42:315–325. [PubMed: 12899503]
15. Liu SK, Coackley C, Krause M, et al. A novel poly (ADP-ri-bose) polymerase inhibitor, ABT-888, radiosensitizes malignant human cell lines under hypoxia. Radiother Oncol. 2008; 88:258–268. [PubMed: 18456354]
16. Robertson KA, Bullock HA, Xu Y, et al. Altered expression of Ape1/ref-1 in germ cell tumors and overexpression in NT2 cells confers resistance to bleomycin and radiation. Cancer Res. 2001; 61:2220. [PubMed: 11280790]
17. Dunne AL, Mothersill C, Robson T, et al. Radiosensitization of colon cancer cell lines by docetaxel: Mechanisms of action. Oncol Res. 2004; 14:447–454. [PubMed: 15490976]
18. Chithrani BD, Ghazani AA, Chan WC. Determining the size and shape dependence of gold nanoparticle uptake into mammalian cells. Nano Lett. 2006; 6:662–668. [PubMed: 16608261]
19. Patra HK, Banerjee S, Chaudhuri U, et al. Cell selective response to gold nanoparticles. Nanomedicine. 2007; 3:111–119. [PubMed: 17572353]
20. Ito S, Miyoshi N, Degraff GW, et al. Enhancement of 5-amino-levulinic acid-induced oxidative stress on two cancer cell lines by gold nanoparticles. Free Radic Res. 2009; 43:1214–1224. [PubMed: 19905984]
21. Chithrani DB, Jelveh S, Jalali F, et al. Gold nanoparticles as radiation sensitizers in cancer therapy. Radiat Res. 2010; 173(6):719–728. [PubMed: 20518651]
22. Liu CJ, Wang CH, Chen ST, et al. Enhancement of cell radiation sensitivity by pegylated gold nanoparticles. Phys Med Biol. 2010; 55:931–945. [PubMed: 20090183]

23. Prise KM, Schettino G, Folkard M, et al. New insights on cell death from radiation exposure. Lancet Oncol. 2005; 6:520–528. [PubMed: 15992701]
24. Bonner JA, Harari PM, Giralt J, et al. Radiotherapy plus cetuximab for squamous-cell carcinoma of the head and neck. N Engl J Med. 2006; 354:567–578. [PubMed: 16467544]
25. McKeown S, Hejmadi M, McIntyre I, et al. AQ4N: An alkylaminoanthraquinone N-oxide showing bioreductive potential and positive interaction with radiation in vivo. Br J Cancer. 1995; 72:76. [PubMed: 7599069]
26. Anai S, Goodison S, Shiverick K, et al. Knock-down of bcl-2 by antisense oligodeoxynucleotides induces radiosensitization and inhibition of angiogenesis in human PC-3 prostate tumor xenografts. Mol Cancer Therapeutics. 2007; 6:101.
27. Roa W, Zhang X, Guo L, et al. Gold nanoparticle sensitize radiotherapy of prostate cancer cells by regulation of the cell cycle. Nanotechnology. 2009; 20:375101. [PubMed: 19706948]
28. Mahmutoglu I, Scheulen ME, Kappus H. Oxygen radical formation and DNA damage due to enzymatic reduction of bleomycin-fe (III). Arch Toxicol. 1987; 60:150–153. [PubMed: 2441682]
29. Wallach-Dayan SB, Izbicki G, Cohen PY, et al. Bleomycin initiates apoptosis of lung epithelial cells by ROS but not by Fas/ FasL pathway. Am J Physiol Lung Cell Mol Physiol. 2006; 290:L790. [PubMed: 16306138]
30. Libutti S, Paciotti G, Myer L, et al. Results of a completed phase I clinical trial of CYT-6091: A pegylated colloidal gold-TNF nanomedicine. ASCO Meeting Abstracts. 2009; 27:15S. 3586.

Europe PMC Funders Author Manuscripts

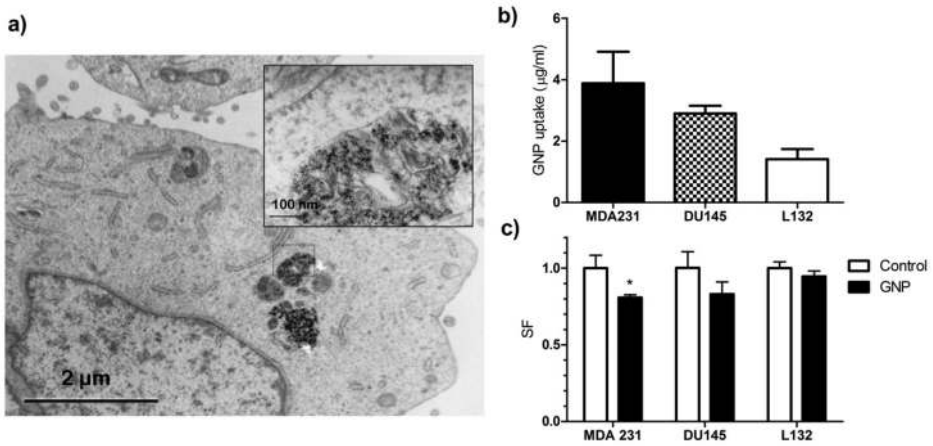

Fig. 1.

Gold nanoparticle cellular uptake and toxicity. (a) Transmission electron microscopy (TEM) of 12 μM gold nanoparticle (GNP) uptake in MDA-MB-231 cells after 24 h. GNPs were located in cytoplasmic lysosomes. (b) Inductively coupled plasma–atomic emission spectroscopy (ICP-AES) quantification of intracellular gold shows greatest uptake in MDA-MB-231 cells. (c) Clonogenic survival of cells exposed to 12 μM GNP for 24 h. Colony formation was reduced by 19.4% in MDA-MB-231 cells (*$p = 0.04$).

Europe PMC Funders Author Manuscripts

Europe PMC Funders Author Manuscripts

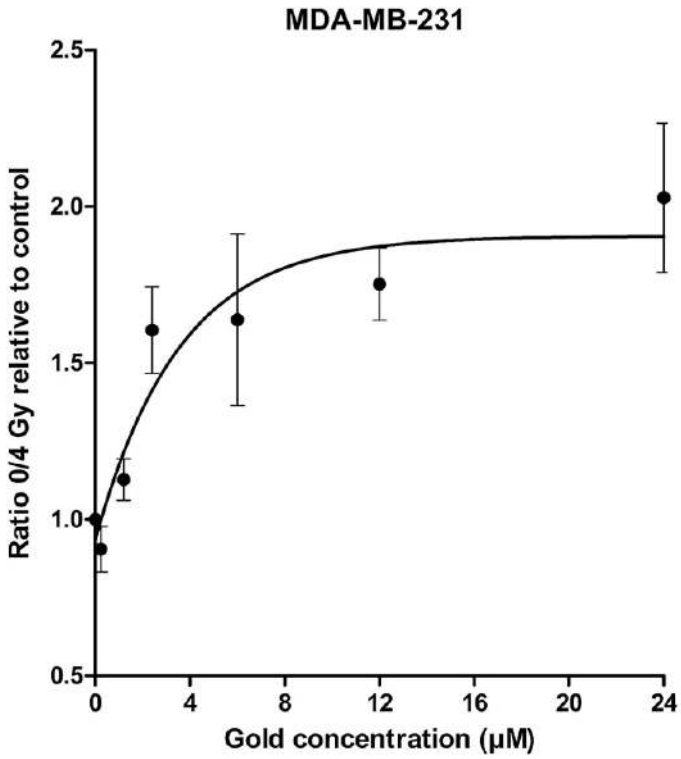

Fig. 2.

Radiosensitization with increasing gold nanoparticle (GNP) concentration. MDA-MB-231 cells were exposed to GNPs for 24 h. Surviving fraction at 4 Gy (SF_4) was determined for control and GNP-exposed cells. The ratio of SF_4 control: SF_4 GNP for each concentration was calculated. The SF_4 ratio increased with GNP concentration up to 12 μM. A concentration of 12 μM was used for all other radiation experiments.

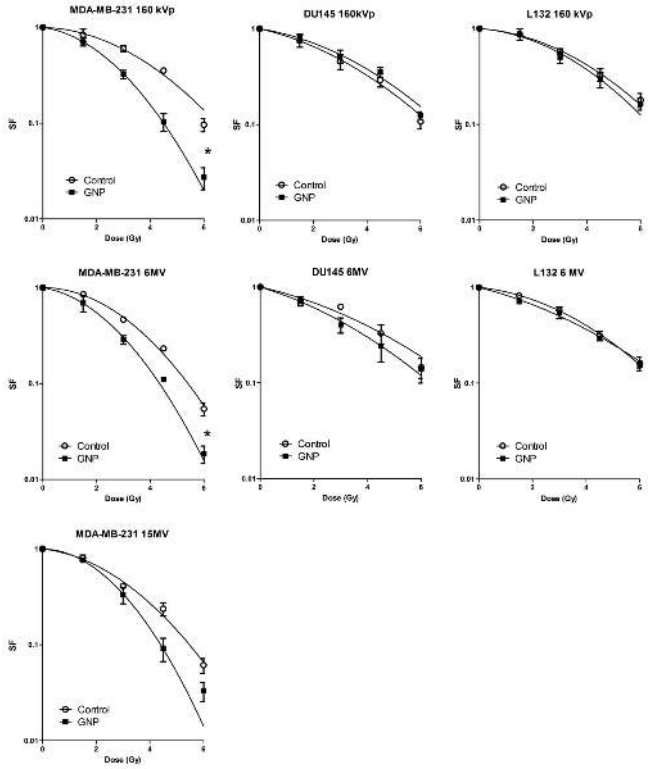

Fig. 3.

Radiation dose response curves for three cell lines with gold nanoparticles (GNPs) at increasing photon energies. The sensitizer enhancement ratio (SER) in MDA-MB-231 cells at 160 kVp, 6 MV, and 15 MV photon energies were 1.41, 1.29, and 1.16, respectively. Statistically significant differences in mean inactivation dose (MID) as defined by the area under the curve are shown (*).

Europe PMC Funders Author Manuscripts

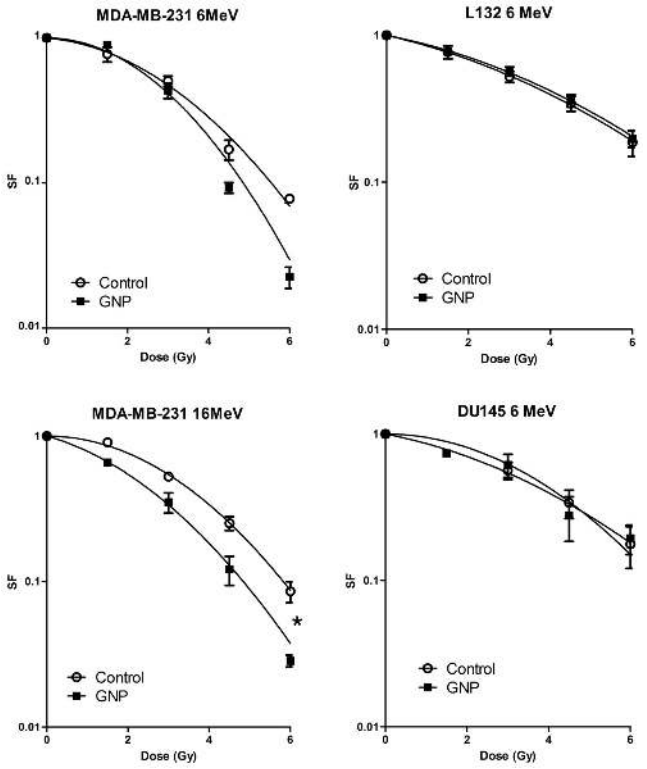

Fig. 4.
Radiation dose response curves for three cell lines exposed to 12 μM gold nanoparticles (GNPs) for 24 h at MV electron energies.

Europe PMC Funders Author Manuscripts

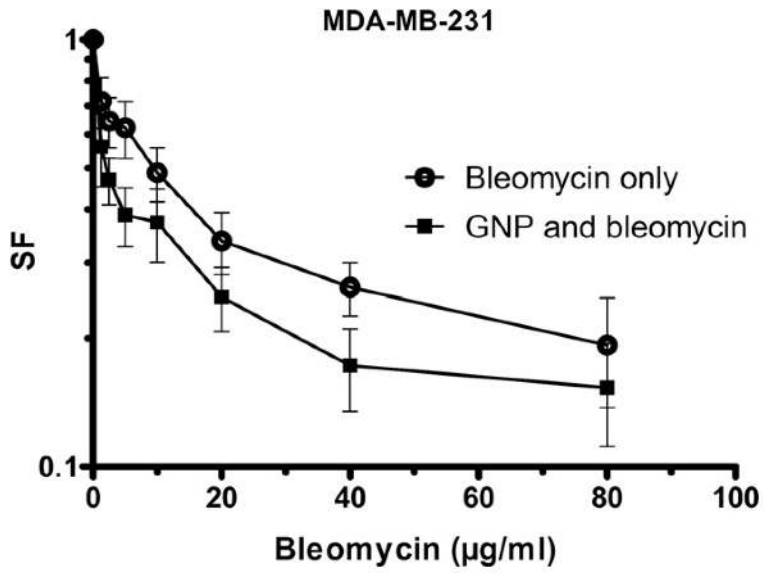

Fig. 5.

Gold nanoparticle (GNP) chemosensitization with the radiomimetic agent, bleomycin. MDA-MB-231 cells were treated with 12 μM 1.9 nm GNPs for 24 h. Mean inactivation doses (MIDs) were calculated (bleomycin only, 25.52 μg/mL; bleomycin and GNP, 18.44 μg/mL). The sensitizer enhancement ratio (SER) was calculated as the MID ratio yielding a value of 1.38.

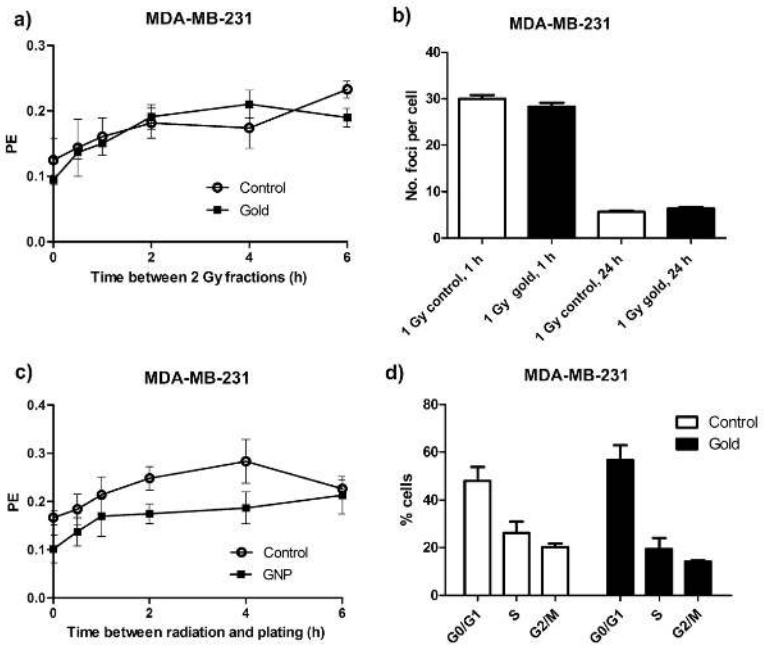

Fig. 6.

DNA repair, double-strand break (DSB) formation, and cell-cycle analysis in cells treated with gold nanoparticles (GNPs). (a) Split dose recovery in MDA-MB-231 cells. Cells were treated with two 2-Gy fractions of 160 kVp X-rays at increasing time intervals. Plating efficiency (PE) increased as time between fractions increased, indicating similar repair rates. (b) Cells were treated with 4 Gy 160 kVp X-rays and time to plating was increased. Reduced PE at time 0 in the GNP-exposed group indicated radiosensitization; however, the rate of increase in PE with time in both groups is similar, suggesting no inhibition of DNA repair. (c) DSB formation measured with 53BP1 foci. No significant increase in foci formation was observed in cells exposed to GNP for 24 h and treated with 1 Gy 160 kVp X-rays when fixed at 1 h or 24 h. (d) Cell-cycle analysis in cells exposed to GNPs. No accumulation of cells in the radiosensitive G2/M phase of the cell cycle was observed.

Europe PMC Funders Author Manuscripts

Europe PMC Funders Author Manuscripts

Table 1

Table of SERs, α, β, and SF_4 values for MDA-MB-231 cells with photons and electrons

		MDA-MB-231					DU145	L132
Radiation energy	**Condition**	**α [Gy^{-1}]**	**β [Gy^{-2}]**	**SF_4**	**SER**	***p***	**SER**	**SER**
160 kVp photons	Control	0.019 ± 0.025	0.052 ± 0.007	0.386	1.41	0.005	0.92	1.05
	GNP	0.091 ± 0.031	0.093 ± 0.011	0.15				
6 MV photons	Control	0.002 ± 0.022	0.079 ± 0.007	0.28	1.29	0.002	1.13	1.08
	GNP	0.104 ± 0.040	0.098 ± 0.011	0.12				
15 MV photons	Control	0.083 ± 0.027	0.059 ± 0.008	0.27	1.16	0.19		
	GNP	0.061 ± 0.050	0.121 ± 0.018	0.16				
6 MeV electrons	Control	0.05 ± 0.002	0.055 ± 0.008	0.029	1.04	0.62	1.12	0.97
	GNP	−0.088 ± 0.034	0.128 ± 0.013	0.18				
16 MeV electrons	Control	−0.038 ± 0.027	0.079 ± 0.008	0.34	1.35	0.01		
	GNP	0.180 ± 0.036	0.015 ± 0.012	0.18				

Abbreviations: GNP = gold nanoparticle; SER = sensitizer enhancement ratio.

SERs are shown for DU145 and L132 cell lines.

Int J Radiat Oncol Biol Phys. Author manuscript; available in PMC 2011 August 01.